Appendix

A. Proof of Theorem 1

Consider $\mathbf{B}$ admits SVD as $\mathbf{U_B\Sigma_B V_B^\top}$. The first term of problem (13) can be rewritten as

$$\frac{1}{2}\|\mathbf{B}-\mathbf{Z}\|_F^2=\frac{1}{2}\left(\|\mathbf{B}\|_F^2-2\langle\mathbf{B},\mathbf{Z}\rangle+\|\mathbf{Z}\|_F^2\right). \tag{17}$$

According to Von Neumann's trace inequality, we have

$$\begin{aligned}\langle\mathbf{B},\mathbf{Z}\rangle =&\mathrm{tr}(\mathbf{B}^\top\mathbf{Z})\\ =&\mathrm{tr}(\mathbf{V_B\Sigma_B U_B^\top Z})\\ =&\mathrm{tr}(\mathbf{\Sigma_B U_B^\top Z V_B})\\ \le&\sum_{i=1}^n\sigma_i(\mathbf{B})\cdot\sigma_i(\mathbf{Z})\cdot\sigma_i(\mathbf{U_B^\top V_B}) \qquad (18)\\ =&\sum_{i=1}^n\sigma_i(\mathbf{B})\cdot\sigma_i(\mathbf{Z}). \qquad (19)\end{aligned}$$

The equality of (18) occurs if and only if

$$\mathbf{U_B}=\mathbf{U_Z},\mathbf{V_B}=\mathbf{V_Z}. \tag{20}$$

Therefore, problem (13) can be rewritten as follows:

$$\begin{aligned}&\arg\min_{\mathbf{B}}\frac{1}{2}\|\mathbf{B}-\mathbf{Z}\|_F^2+\lambda\|\mathbf{B}\|_{t,*-F}\\ =&\arg\min_{\mathbf{B}}\frac{1}{2}\|\mathbf{B}\|_F^2-\sum_{i=1}^n\sigma_i(\mathbf{B})\sigma_i(\mathbf{Z})+\frac{1}{2}\|\mathbf{Z}\|_F^2\\ &+\lambda\Big(\sum_{i=t+1}^n\sigma_i(\mathbf{B})-\big(\sum_{i=t+1}^n\sigma_i(\mathbf{B})^2\big)^{\frac{1}{2}}\Big)\\ =&\arg\min_{\mathbf{B}}\sum_{i=1}^n\Big(\frac{1}{2}\sigma_i(\mathbf{B})^2-\sigma_i(\mathbf{B})\sigma_i(\mathbf{Z})\Big)+\sum_{i=t+1}^n\Big(\frac{1}{2}\sigma_i(\mathbf{B})^2\\ &-\sigma_i(\mathbf{B})\sigma_i(\mathbf{Z})+\lambda\sigma_i(\mathbf{B})\Big)-\lambda\Big(\sum_{i=t+1}^n\sigma_i(\mathbf{B})^2\Big)^{\frac{1}{2}}. \qquad (21)\end{aligned}$$

Therefore, the original problem (13) has been equivalently transformed into the combination of independent quadratic equations for each $\sigma_i(\mathbf{B})$. Let $F(\boldsymbol{\sigma}(\mathbf{B}))$ denote the objective function of (21). The minimum of F, denoted as ϱ_i^*, is given by

$$\frac{\partial F}{\partial\sigma_i(\mathbf{B})}=0. \tag{22}$$

When $0\le i<t+1$, it is trivial to obtain

$$\varrho_i^*=\sigma_i(\mathbf{Z}). \tag{23}$$

When $t+1\le i\le n$, equation (22) is expressed as

$$\Big(1-\frac{\lambda}{\|\boldsymbol{\sigma}(\mathbf{B})\|_2}\Big)\boldsymbol{\sigma}(\mathbf{B})=\boldsymbol{\sigma}(\mathbf{Z})-\lambda. \tag{24}$$

Let $\mathbf{r}=[0,\dots,0,\sigma_{t+1}(\mathbf{Z}),\dots,\sigma_T(\mathbf{Z})]^\top\in\mathbb{R}^n$ and $\mathcal{S}_\lambda(\mathbf{r})_i=\max(\mathbf{r}_i-\lambda,0)$, the solution of (24) is

$$\varrho_i^*=\Big(1+\frac{\lambda}{\|\mathcal{S}_\lambda(\mathbf{r})\|_2}\Big)\cdot\mathcal{S}_\lambda(\sigma_i(\mathbf{Z})). \tag{25}$$

Combining (23) and (24), the minimum of F is obtained at

$$\varrho_i^*=\begin{cases}\sigma_i(\mathbf{Z}), & \text{if } 0\le i<t+1,\\ \big(1+\frac{\lambda}{\|\mathcal{S}_\lambda(\mathbf{r})\|_2}\big)\mathcal{S}_\lambda(\sigma_i(\mathbf{Z})), & \text{if } t+1\le i<n+1.\end{cases} \tag{26}$$

Therefore, the optimal solution of problem (13) is

$$\mathbf{B}^*=\mathbf{U_Z}\mathrm{Diag}(\varrho^*)\mathbf{V_Z^\top}. \tag{27}$$

□

B. Proof of Theorem 2

The sequence of dual variable $\{\mathbf{D}_k\}$ is upper bounded since

$$\begin{aligned}\|\mathbf{D}_{k+1}\|_F^2&=\|\mathbf{D}_k+\psi_k(\mathbf{X}_{k+1}-\mathbf{B}_k)\|_F^2\\ &=\psi_k^2\|(\psi^{-1}\mathbf{D}_k+\mathbf{X}_{k+1})-\mathbf{B}_{k+1}\|_F^2\\ &=\psi_k^2\|\mathbf{U}_{\mathbf{Z}_k}\mathbf{\Sigma}_{\mathbf{Z}_k}\mathbf{V}_{\mathbf{Z}_k}^\top-\mathbf{U}_{\mathbf{Z}_k}\mathrm{Diag}(\varrho^*)\mathbf{V}_{\mathbf{Z}_k}^\top\|_F^2\\ &=\psi_k^2\sum_{i=t+1}^n(\sigma_i(\mathbf{Z}_k)-\varrho_i^*)^2.\end{aligned} \tag{28}$$

If $\sigma_i(\mathbf{Z}_k)>\lambda/\psi_k$, $\varrho_i^*=(1+\frac{\lambda/\psi_k}{\|\mathcal{S}_{\lambda/\psi_k}(\mathbf{r})\|_2})\cdot(\sigma_i(\mathbf{Z}_k)-\lambda/\psi_k)$. Let $\theta=1+\frac{\lambda/\psi_k}{\|\mathcal{S}_{\lambda/\psi_k}(\mathbf{r})\|_2}$. We have $\sigma_i(\mathbf{Z}_k)-\varrho_i^*=(1-\theta)\sigma_i(\mathbf{Z}_k)+\theta\lambda/\psi_k<\lambda/\psi_k$. If $\sigma_i(\mathbf{Z}_k)\le\lambda/\psi_k$, $\varrho_i^*=0$. We have $\boldsymbol{\sigma}_i(\mathbf{Z}_k)-\varrho_i^*=\sigma_i(\mathbf{Z}_k)\le\lambda/\psi_k$. Overall, we have $\sigma_i(\mathbf{Z}_k)-\varrho_i^*\le\lambda/\psi_k$. Then we can deduce

$$\|\mathbf{D}_{k+1}\|_F^2\le\psi_k^2\sum_{i=t+1}^n(\lambda/\psi_k)^2=\lambda^2(T-t). \tag{29}$$

Since $\{\mathbf{D}_k\}$ is upper bounded, $\{\mathbf{D}_{k+1}-\mathbf{D}_k\}$ is upper bounded, i.e., $\exists M>0,\forall k\ge0,\|\mathbf{D}_{k+1}-\mathbf{D}_k\|_F\le M$. According to the squeeze theorem, we have

$$\begin{aligned}0\le&\lim_{k\to\infty}\|\mathbf{X}_{k+1}-\mathbf{B}_{k+1}\|_F\\ &=\lim_{k\to\infty}\psi_k^{-1}\|\mathbf{D}_{k+1}-\mathbf{D}_k\|_F\le\lim_{k\to\infty}\frac{M}{\psi_k}=0.\end{aligned} \tag{30}$$

Therefore, (a) is proved.

The objective function in (4) can be transformed as follows

$$\begin{aligned}&\|\mathbf{C}(\mathbf{Y}-\mathbf{X})\|_F^2+\lambda\|\mathbf{B}\|_{t,*-F}\\ =&\mathcal{L}_{\psi_{k-1}}(\mathbf{X}_k,\mathbf{B}_k,\mathbf{D}_{k-1})-\langle\mathbf{D}_{k-1},\mathbf{X}_k-\mathbf{B}_k\rangle\\ &-\psi_{k-1}/2\|\mathbf{X}_k-\mathbf{B}_k\|_F^2\\ =&\mathcal{L}_{\psi_{k-1}}(\mathbf{X}_k,\mathbf{B}_k,\mathbf{D}_{k-1})-\langle\mathbf{D}_{k-1},(\mathbf{D}_k-\mathbf{D}_{k-1})/\psi_k\rangle\\ &-\psi_{k-1}/2\|(\mathbf{D}_k-\mathbf{D}_{k-1})/\psi_k\|_F^2\\ =&\mathcal{L}_{\psi_{k-1}}(\mathbf{X}_k,\mathbf{B}_k,\mathbf{D}_{k-1})+(2\psi_k)^{-1}(\|\mathbf{D}_{k-1}-\mathbf{D}_k\|_F^2).\end{aligned} \tag{31}$$

The augmented Lagrangian term of (31) satisfies

$$\mathcal{L}_{\psi_{k-1}}(\mathbf{X}_k,\mathbf{B}_k,\mathbf{D}_{k-1})\le\mathcal{L}_{\psi_{k-1}}(\mathbf{X}_{k-1},\mathbf{B}_{k-1},\mathbf{D}_{k-1}), \tag{32}$$

since the global optimum of $\mathbf{X}$ and $\mathbf{B}$ can be got from step 3 and 4 in Algorithm 2. Consequently, we have

$$\begin{aligned}&\mathcal{L}_{\psi_k}(\mathbf{X}_k,\mathbf{B}_k,\mathbf{D}_k)\\ =&\mathcal{L}_{\psi_{k-1}}(\mathbf{X}_k,\mathbf{B}_k,\mathbf{D}_{k-1})+\langle\mathbf{D}_k-\mathbf{D}_{k-1},\mathbf{X}_k-\mathbf{B}_k\rangle\\ &+(\psi_k-\psi_{k-1})/2\|\mathbf{X}_k-\mathbf{B}_k\|_F^2\\ =&\mathcal{L}_{\psi_{k-1}}(\mathbf{X}_k,\mathbf{B}_k,\mathbf{D}_{k-1})+\langle\mathbf{D}_k-\mathbf{D}_{k-1},\frac{\mathbf{D}_k-\mathbf{D}_{k-1}}{\psi_k}\rangle\\ &+(\psi_k-\psi_{k-1})/(2\psi_{k-1}^2)\|\mathbf{D}_k-\mathbf{D}_{k-1}\|_F^2\\ \le&\mathcal{L}_{\psi_{k-1}}(\mathbf{X}_k,\mathbf{B}_k,\mathbf{D}_{k-1})+\frac{\psi_k+\psi_{k-1}}{2\psi_{k-1}^2}\cdot M^2\\ \le&\mathcal{L}_{\psi_0}(\mathbf{X}_1,\mathbf{B}_1,\mathbf{D}_0)+M^2\textstyle\sum_{k=1}^\infty\frac{\psi_k+\psi_{k-1}}{2\psi_{k-1}^2}\\ =&\mathcal{L}_{\psi_0}(\mathbf{X}_1,\mathbf{B}_1,\mathbf{D}_0)+M^2\textstyle\sum_{k=1}^\infty\frac{\varphi+1}{2\varphi^{k-1}\psi_0}\\ \le&\mathcal{L}_{\psi_0}(\mathbf{X}_1,\mathbf{B}_1,\mathbf{D}_0)+\frac{M^2}{\psi_0}\textstyle\sum_{k=1}^\infty\frac{1}{\varphi^{k-2}},\end{aligned}$$

where the last inequality holds as $\varphi+1<2\varphi$. Since $\sum_{k=0}^\infty\frac{1}{\varphi^{k-2}}<\infty$, $\{\mathcal{L}_{\psi_{k-1}}(\mathbf{X}_k,\mathbf{B}_k,\mathbf{D}_{k-1})\}$ is upper bounded. Therefore, the objective function in (4) is upper bounded. Therefore, both $\|\mathbf{C}(\mathbf{Y}-$

$\mathbf{X})\|_F^2$ and $\lambda\|\mathbf{B}\|_{t,*-F}$ are upper bounded since both them are positive. Then we can prove b) and c).

$$
\begin{aligned}
&\lim_{k\to\infty}\|\mathbf{X}_{k+1}-\mathbf{X}_k\|_F\\
=&\lim_{k\to\infty}\|(\mathbf{C}^\top\mathbf{C}+\frac{\psi_k}{2}\mathbf{I})^{-1}(\mathbf{C}^\top\mathbf{C}\mathbf{Y}+\frac{\psi_k}{2}\mathbf{B}_k-\frac{1}{2}\mathbf{D}_k)\\
&\quad-\frac{1}{\psi_{k-1}}(\mathbf{D}_k-\mathbf{D}_{k-1})-\mathbf{B}_k\|_F\\
=&\lim_{k\to\infty}\|(\mathbf{C}^\top\mathbf{C}+\frac{\psi_k}{2}\mathbf{I})^{-1}(\mathbf{C}^\top\mathbf{C}\mathbf{Y}-\mathbf{C}^\top\mathbf{C}\mathbf{B}_k-\frac{1}{2}\mathbf{D}_k)\\
&\quad-\frac{1}{\psi_{k-1}}(\mathbf{D}_k-\mathbf{D}_{k-1})\|_F\\
=&\lim_{k\to\infty}\|(\mathbf{C}^\top\mathbf{C}+\frac{\psi_k}{2}\mathbf{I})^{-1}\Big(\mathbf{C}^\top\mathbf{C}\mathbf{Y}-\mathbf{C}^\top\mathbf{C}(\mathbf{X}_k\\
&\quad+\frac{1}{\psi_{k-1}}(\mathbf{D}_{k-1}-\mathbf{D}_k))-\frac{1}{2}\mathbf{D}_k\Big)-\frac{1}{\psi_{k-1}}(\mathbf{D}_k-\mathbf{D}_{k-1})\|_F\\
=&\lim_{k\to\infty}\|(\mathbf{C}^\top\mathbf{C}+\frac{\psi_k}{2}\mathbf{I})^{-1}(\mathbf{C}^\top\mathbf{C}(\mathbf{Y}-\mathbf{X}_k)-\mathbf{C}^\top\mathbf{C}\frac{1}{\psi_{k-1}}\mathbf{D}_{k-1}\\
&\quad+(\frac{1}{\psi_{k-1}}\mathbf{C}^\top\mathbf{C}-\frac{1}{2}\mathbf{I})\mathbf{D}_k)\|_F\\
\leq&\lim_{k\to\infty}\|(\mathbf{C}^\top\mathbf{C}+\frac{\psi_k}{2}\mathbf{I})^{-1}\mathbf{C}^\top\mathbf{C}(\mathbf{Y}-\mathbf{X}_k)\|_F\\
&\quad+\|(\mathbf{C}^\top\mathbf{C}+\frac{\psi_k}{2}\mathbf{I})^{-1}\mathbf{C}^\top\mathbf{C}\frac{1}{\psi_{k-1}}\mathbf{D}_{k-1}\|_F\\
&\quad+\|(\mathbf{C}^\top\mathbf{C}+\frac{\psi_k}{2}\mathbf{I})^{-1}(\frac{1}{\psi_{k-1}}\mathbf{C}^\top\mathbf{C}-\frac{1}{2}\mathbf{I})\mathbf{D}_k\|_F\\
=&0.
\end{aligned}
\tag{33}
$$

$$
\begin{aligned}
&\lim_{k\to\infty}\|\mathbf{B}_{k+1}-\mathbf{B}_k\|_F\\
=&\lim_{k\to\infty}\|\frac{1}{\psi_k}(\mathbf{D}_k-\mathbf{D}_{k+1})+\mathbf{X}_{k+1}-\mathbf{B}_k\|_F\\
=&\lim_{k\to\infty}\|(\mathbf{X}_k+\frac{1}{\psi_{k-1}}\mathbf{D}_{k-1}-\mathbf{B}_k)+(\mathbf{X}_{k+1}-\mathbf{X}_k)\\
&\quad-\frac{1}{\psi_{k-1}}\mathbf{D}_{k-1}+\frac{1}{\psi_k}(\mathbf{D}_k-\mathbf{D}_{k+1})\|_F\\
\leq&\lim_{k\to\infty}\frac{1}{\psi_{k-1}}\|\mathbf{D}_k\|_F+\|\mathbf{X}_{k+1}-\mathbf{X}_k\|_F\\
&\quad+\frac{1}{\psi_{k-1}}\|\mathbf{D}_{k-1}\|_F-\frac{1}{\psi_k}\|\mathbf{D}_k+\mathbf{D}_{k+1}\|_F\\
=&0.
\end{aligned}
\tag{34}
$$

□

C. More Denoising Results

Under noise level $(20, 35, 5)$, we display "kodim01", "kodim03", "kodim04", and "kodim16", shown in Fig. 5 $\sim$ Fig. 8. Under noise level $(30, 10, 50)$, we display "kodim09", "kodim11", "kodim13", and "kodim14", shown in Fig. 9 $\sim$ Fig. 12.

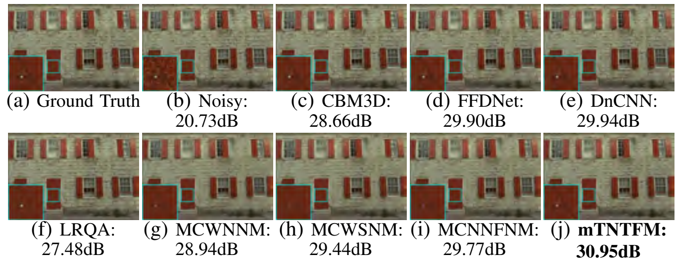

Fig. 5. Denoised results on "kodim01.png" under the noise level $(\nu_r, \nu_g, \nu_b) = (20, 35, 5)$.

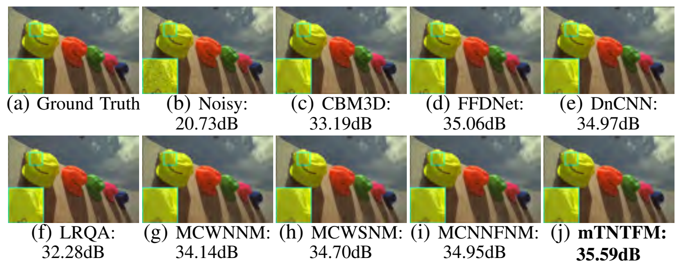

Fig. 6. Denoised results on "kodim03.png" under the noise level $(\nu_r, \nu_g, \nu_b) = (20, 35, 5)$.

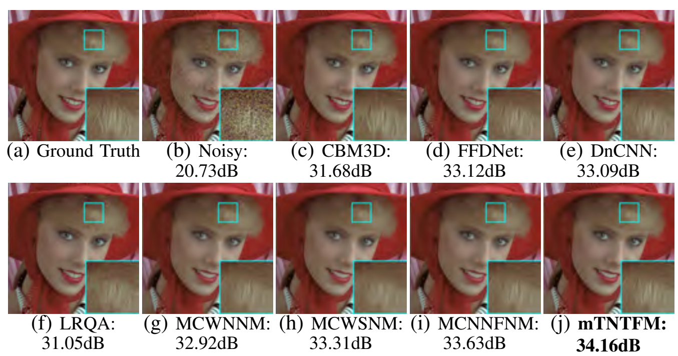

Fig. 7. Denoised results on "kodim04.png" under the noise level $(\nu_r, \nu_g, \nu_b) = (20, 35, 5)$.

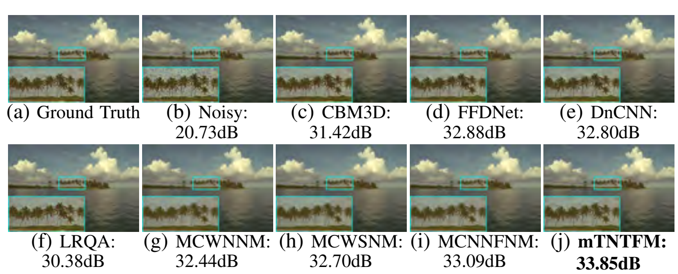

Fig. 8. Denoised results on "kodim16.png" under the noise level $(\nu_r, \nu_g, \nu_b) = (20, 35, 5)$.

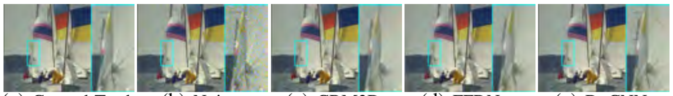

(a) Ground Truth | (b) Noisy: 17.46dB | (c) CBM3D: 31.17dB | (d) FFDNet: 31.03dB | (e) DnCNN: 31.89dB

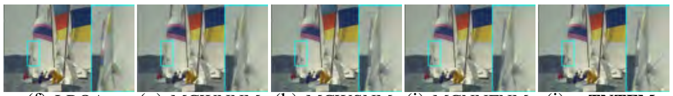

(f) LRQA: 31.59dB | (g) MCWNNM: 32.08dB | (h) MCWSNM: 32.57dB | (i) MCNNFNM: 32.84dB | (j) **mTNTFM: 32.91dB**

Fig. 9. Denoised results on "kodim09.png" under the noise level $(\nu_r, \nu_g, \nu_b) = (30, 10, 50)$.

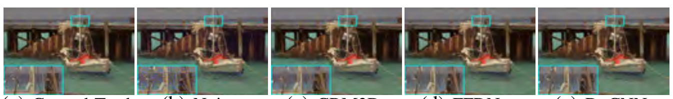

(a) Ground Truth | (b) Noisy: 17.46dB | (c) CBM3D: 28.88dB | (d) FFDNet: 29.08dB | (e) DnCNN: 29.67dB

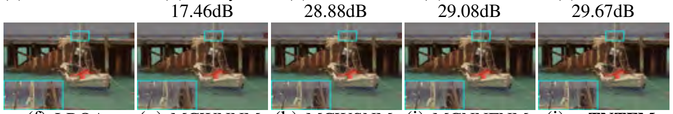

(f) LRQA: 28.91dB | (g) MCWNNM: 29.60dB | (h) MCWSNM: 29.84dB | (i) MCNNFNM: 30.09dB | (j) **mTNTFM: 30.16dB**

Fig. 10. Denoised results on "kodim11.png" under the noise level $(\nu_r, \nu_g, \nu_b) = (30, 10, 50)$.

(a) Ground Truth | (b) Noisy: 17.46dB | (c) CBM3D: 25.44dB | (d) FFDNet: 25.87dB | (e) DnCNN: 26.18dB

(f) LRQA: 24.87dB | (g) MCWNNM: 25.96dB | (h) MCWSNM: 26.25dB | (i) MCNNFNM: 26.25dB | (j) **mTNTFM: 26.42dB**

Fig. 11. Denoised results on "kodim13.png" under the noise level $(\nu_r, \nu_g, \nu_b) = (30, 10, 50)$. The highlighted windows are omitted.

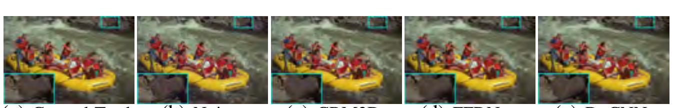

(a) Ground Truth | (b) Noisy: 17.46dB | (c) CBM3D: 27.67dB | (d) FFDNet: 28.12dB | (e) DnCNN: 28.62dB

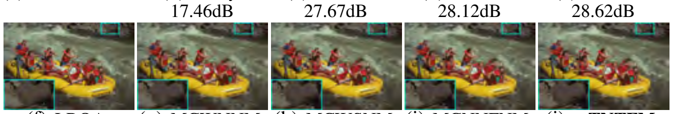

(f) LRQA: 27.87dB | (g) MCWNNM: 28.57dB | (h) MCWSNM: 28.75dB | (i) MCNNFNM: 29.00dB | (j) **mTNTFM: 29.08dB**

Fig. 12. Denoised results on "kodim14.png" under the noise level $(\nu_r, \nu_g, \nu_b) = (30, 10, 50)$.